EFFECTS OF CANNABIDIOL (CBD) ON DEVELOPMENT OF THE LIVER AND THYROID OF WOOD FROGS (*LITHOBATES SYLVATICA*)

A Report of a Senior Study

by

Bryan Crouser

Major: Biology B.A.

Maryville College

Spring, 2020

Date approved Nov. 17, 2020, by _____

Faculty Supervisor

Date approved Nov. 17, 2020, by _____

Division Chair

ABSTRACT

Cannabidiol (CBD), which is a non-psychoactive phytocannabinoid present in the Cannabis plant, recreational use has recently increased throughout the United States. The purpose of this study was to determine the acute and chronic effects that CBD could have on the development of the liver and thyroid of Wood frogs and (*Lithobates sylvatica*) tadpoles and newly metamorphosed frogs. Both frogs and tadpoles were collected and split into experimental and control groups. Each of the experimental groups were exposed to a normal human dosage (15mg/kg) for a 16-day period. Histology was conducted on the livers and thyroids. In the liver, 20 measurements of hepatocyte height and width were measured per animal in each respective group, and five measurements of hepatocyte density was measured per animal. In the thyroid, five measurements of follicle height and width were measured per animal in each respective group, and 10 measurements of cuboidal epithelial cell height and width were measured per animal in each group. Statistical analysis was performed to determine if there was significant difference in the size of each of the measured areas. CBD exposure statistically ($p<0.05$) reduced height and width of hepatocytes in both frogs and tadpoles, increased density of hepatocytes in both frogs and tadpoles, reduced follicle height and width of tadpoles, increased follicle height of frogs, reduced cuboidal epithelial cell width of tadpoles, and increased cuboidal epithelial cell height of frogs. Thus, CBD did affect the growth of both frogs and tadpoles to a degree, by making the cells smaller. This could be due to an increased amount of mitotic division in the CBD exposed frogs and

tadpoles. Further studies should be done to confirm the possible effects of CBD on the liver and thyroid structure.

ACKNOWLEDGEMENTS

Firstly, I would like to thank Dr. Crain for advising me and guiding me through this process. I would like to thank Dr. Duncan for helping me come up with the idea for this study and also Kelsey Birchfield and Julia Warrick for constant support in the laboratory and for helping the process go faster. I give thanks to my family and friends for continually cheering me on and making sure that I am just simply doing my best. Lastly, I want to thank Maryville College for letting me complete this study and also to use their facilities to complete this project.

TABLE OF CONTENTS

LIST OF TABLES

LIST OF FIGURES

CHAPTER I

INTRODUCTION

Dietary supplements are substances that do not need to be registered or approved by the US Food and Drug Administration (FDA) before they are produced and sold. Over 70% of Americans who take some form of dietary supplement on a daily basis, leading to a business that has a gross profit of well over 28-billion dollars (Ronis 2018). Recently, there has been an increase in the restrictions of dietary supplements. Studies have shown that cross contamination has played a factor especially in muscle building dietary supplements, which has caused individuals to fail doping tests (Mathews 2018). An estimated 14.8% of suppliers for dietary supplements had contamination of hormones and prohormones, which has caused an increase in liver injury reported by the Drug Induced Liver Injury Network from 7% to 20% between 2004 and 2013 (Mathews 2018).

Cannabis is a medicinal plant that contains a complex matrix composed of cannabinoids and terpenoids (Jagannathan 2020). Cannabinoids include a wide variety of different substances (Landmark 2020) including cannabidiol (CBD), which is known as a non-psychoactive phytocannabinoid present in Cannabis (Lazarini-Lopes 2020), the structure of which can be seen in Figure 1. In the past two years, there has been an increase in cannabis legalization in several states in the United States and, as a result, CBD oil businesses have become available for recreational purposes (Hazekamp 2018). With this,

CBD has not had a large amount of experimentation evaluated to determine what the effects are to the human body upon utilization (Khan 2020). CBD use has increased for medicinal purpose including treatments for anxiety, muscle spasticity, chemotherapy-induced nausea and vomiting, and also epilepsy (Sarris 2020). Numerous studies have shown that CBD decreases the symptoms of medical conditions (See Table 1), few studies have examined the negative consequences of the use of CBD (Calcaterra 2020). However, the studies that have shown adverse effects have provided crucial information. One study was performed that gathered up data from all other studies of CBD to examine the risk/benefit. It was found that CBD included many developmental toxicity including: hepatocellular injuries, spermatogenesis reduction, organ weight alterations, male reproductive system alterations, and hypotension. This primarily occurred when dosing was higher than recommended for human pharmacotherapy practices (Huestis 2019).

Previous studies have examined the effects of CBD on the testis. A majority of the studies have shown a decrease in many male characteristics of the reproductive system (Carvalho 2018; see Table 2). However, few studies have examined effects on the liver.

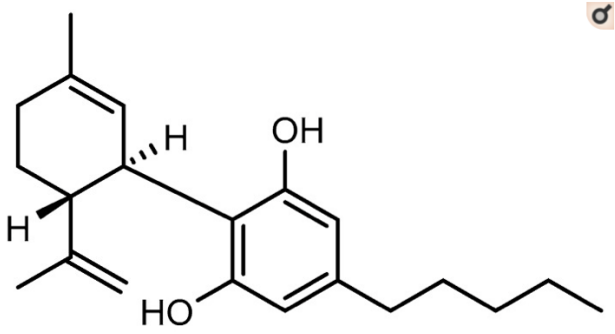

Figure 1: The chemical structure of cannabidiol (from Mabou 2019).

Table 1: Medical conditions that have been affected in positive ways due to the exposure of CDB.

Medical Condition	Effect After	Reference
Substance abuse, and anxiety	The patients started successfully stopping substance abuse (without withdrawal symptoms) and improved with anxiety symptoms	Laczkovics 2020
Dravet Syndrome	The patients started to have less seizures episodes	Lattanzi 2020
Parkinson's Disease	There was a lowering of anxiety along with the amount of tremors	Faria 2020
Schizophrenia	The patients experienced effects of antipsychotic-like and procognitive activities	Kozela 2019
Hypertension	The patients experienced almost full concentration-dependent relaxation	Baranowska-Kuczko 2019

Table 2: The mean and standard deviation of sperm morphology in vas deferens and the presence/position of cytoplasmic droplet in 90 day old swiss mice orally treated to 15 and 30mg kg^{-1} including a control group of CBD (from Carvalho 2018).

Parameter	**Control (n=10)**	**CBD 15 (n=10)**	**CBD 30 (n=10)**
Sperm morphology			
Normal	102.0 ± 26.0	100.0 ± 15.0	95.0 ± 10.0
Head abnormalities	49.0 ± 18.0	60.0 ± 14.0	57.0 ± 16.0
Tail abnormalities	35.0 ± 18.0	36.0 ± 9.0	37.0 ± 18.0
Isolated head	14.0 ± 18.0	4.0 ± 4.0	11.0 ± 10.0
Cytoplasmic droplet			
Absent	91.0 ± 35.0	67.0 ± 20.0	70.0 ± 21.0
Proximal	1.0 ± 1.0	1.0 ± 1.0	0.0 ± 0.0
Medial	104.0 ± 33.0	127.0 ± 22.0	125.0 ± 22.0
Distal	4.0 ± 4.0	5.0 ± 5.0	5.0 ± 5.0

Liver Structure and Function

The liver is considered the largest of the digestive glands, where it serves as a nutrient storage organ and a producer of bile (Vaissi 2017). The cellular structure of the liver is comprised of a functional unit called the lobule (see Figure 2). This is a hexagonal formation

that includes a portal triad, which is the portal vein, hepatic artery, and also the bile duct (Kalra 2018). Each lobule is measured at 1-2mm in diameter and the main component of the lobule are hepatocytes that are separated by endothelium-lined sinusoids (Chandrasoma 1998), shown in Figure 3.

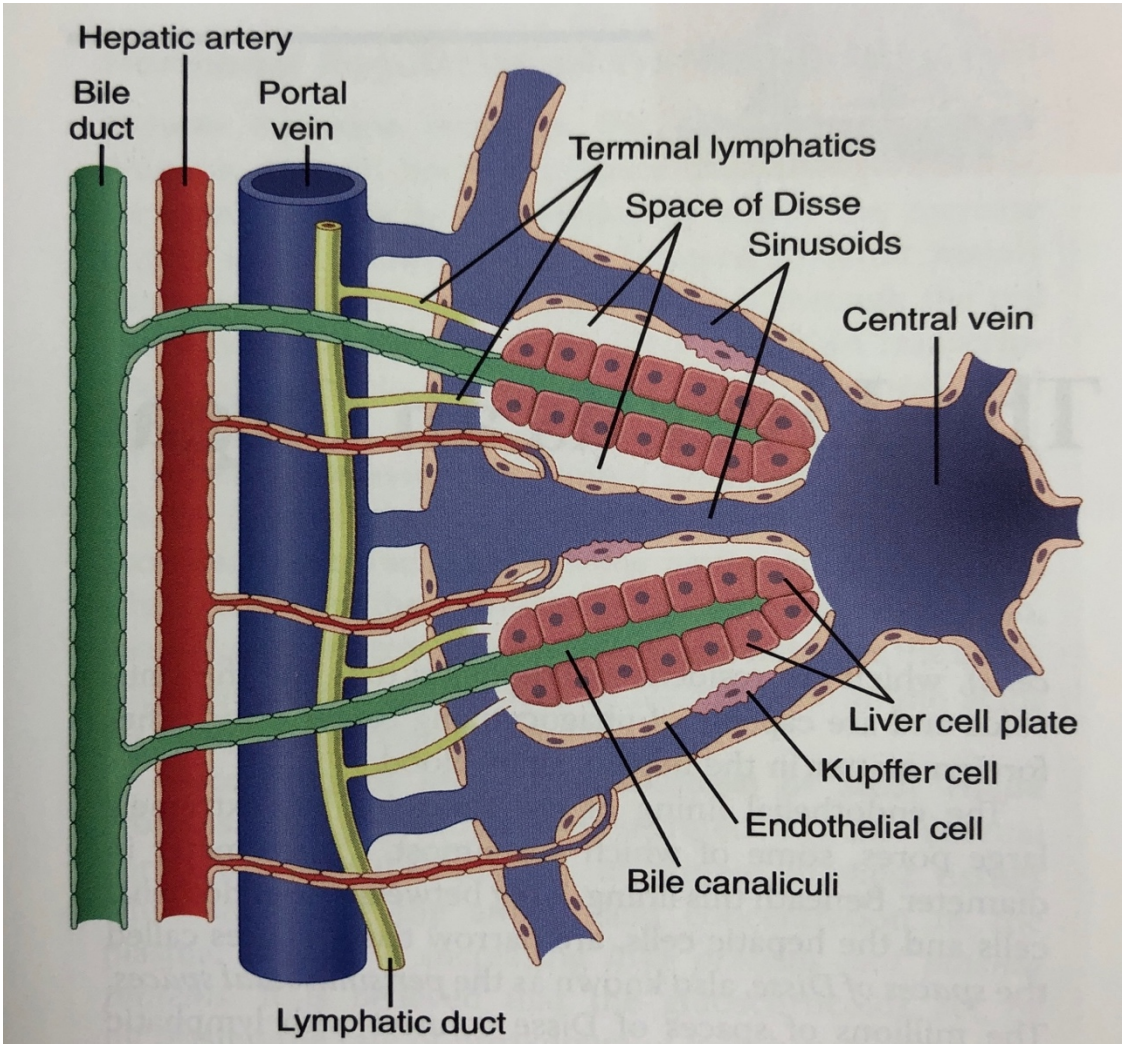

Figure 2: Microscale structure of a human liver (from Hall 2016).

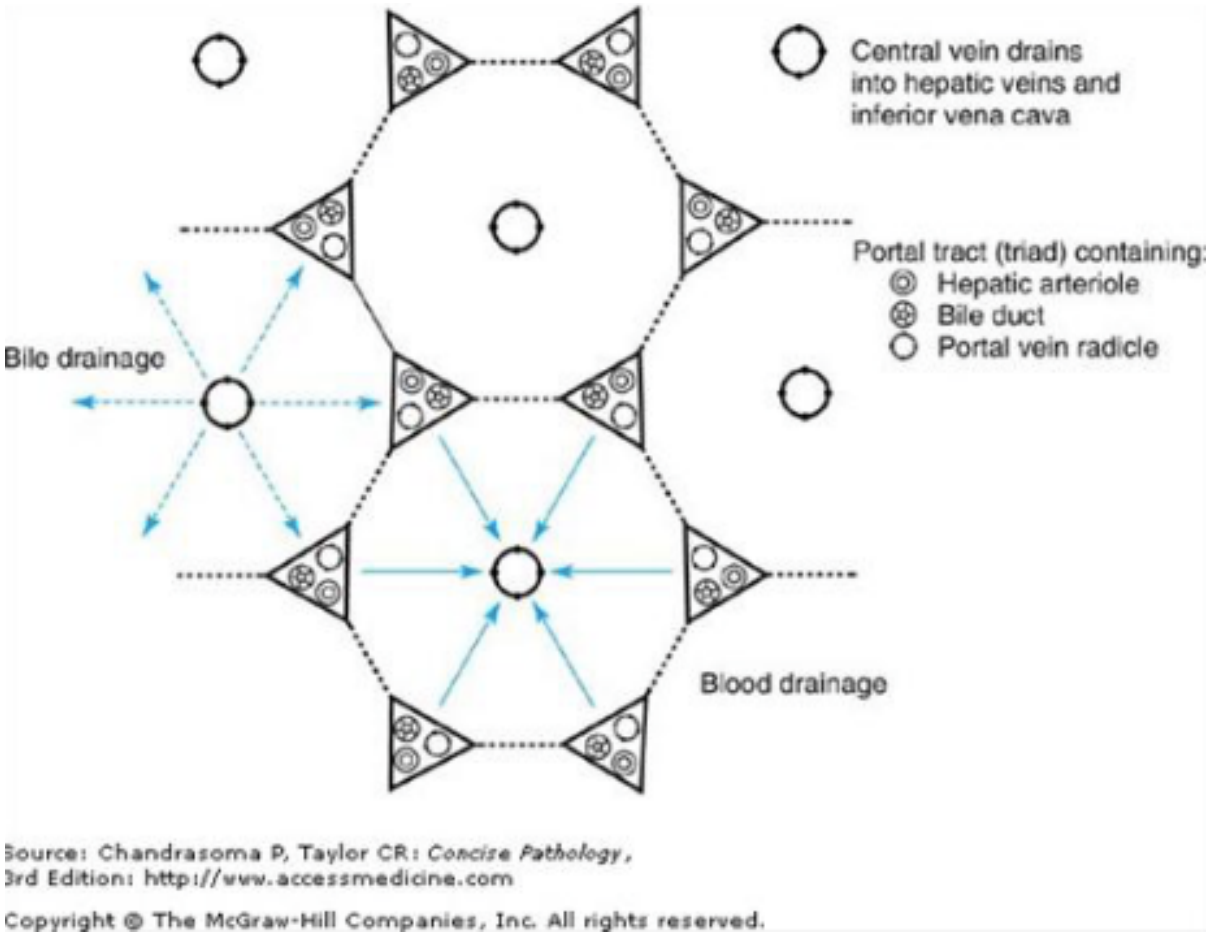

Figure 3: Architecture of the liver lobule, showing the hepatocytes and how sinusoids receive blood from the branches of the portal vein and hepatic artery and go into the central vein (solid lines) and how bile drainage goes towards the portal tracts. (from Chandrasoma 1998).

The various structures of the liver serve distinct functions (see Table 3). Hepatocytes have many different functions depending on what zone is examined. The first zone is where hepatocytes are best at regenerating due to them being able to get oxygenated blood and nutrients easily. Since this area is also high in perfusion, they also play a role in oxidative metabolism, which includes gluconeogenesis, bile formation , and cholesterol formation. The second zone, is what is known as the pericentral region of hepatocytes. Then, the third zone has a role in detoxification, glycolysis, ketogenesis, and also biotransformation of drugs.

However, this zone has low perfusion meaning that it is distant from the portal triad (Kalra 2018).

The liver also acts as a source of bile production, which is important due to bile being a fluid that helps rid material not excreted by the kidney (Chandrasoma 1998). Hepatic bile is then stored in the gallbladder, where it then moves through the bile duct into the duodenum, to emulsify fats (Vaissi 2017). The liver also helps with metabolism, where Hepatocytes aid in the digestion of lipids and is able to free fatty acids from adipose tissue (Chandrasoma 1998).

Another important function of the liver is the metabolism and detoxification of xenobiotics (Trefts 2017). The liver uses two different reactions to be able to transform xenobiotics from a lipophilic form to a hydrophilic form: (1) synthesis of a more hydrophilic solute through oxidation and hydrolysis using mainly cytochrome P450 and (2) conjugation of the metabolites that were created from the first reaction and make them more hydrophilic so that they can be ready for secretion into blood or bile (Kalra 2018).

Table 3: The components of a human liver and their definition/function (from Esrefoglu 2016).

Component	Definition/Function
Bile Duct	Part of the portal triad. Helps aid in the flow of bile from the central vein to the portal space using canaliculi and bile canals
Portal Vein	Part of the portal triad. Contains venous and arterial blood that is then sent to the hepatocytes that are separated by sinusoid capillaries
Hepatocytes	Large polygonal cells rich in organelles including rough and smooth endoplasmic reticulum, several Golgi complexes, mitchodri, etc.
Hepatic Artery	Part of the portal triad. Also, contains venous and arterial blood that is then sent to the hepatocytes.
Central Vein	Is at the center of the lobule and is represented as a large venule where sinusoid capillaries drain.
Sinusoids	Large capillaries lined with a discontinuous endothelium with discontinuous basal lamina, in which blood flows through
Kupffer Cells	Are derived from monocytes and attach to the sinusoidal wall. These are involved in the breakdown senile erythrocytes and harmful materials.

Thyroid Structure and Function

The thyroid gland is responsible for is the production and secretion of the thyroid hormones, triiodothyronine (T_3) and thyroxine (T_4). The thyroid gland in a human is located at the front of the neck, and it is made of two different types of cells, follicular and parafollicular (see Figure 4). The follicular cells are responsible for producing the previously stated thyroid hormones, and these cells also enclose a space called the colloid (Chiasera 2013). The colloid is made up of thyroglobulin (Tg), which is a glycoprotein that is used to produce the thyroid hormones. These follicles are highly vascularized and are surrounded by capillaries, inside of which are red blood cells (DeRuiter 2004).

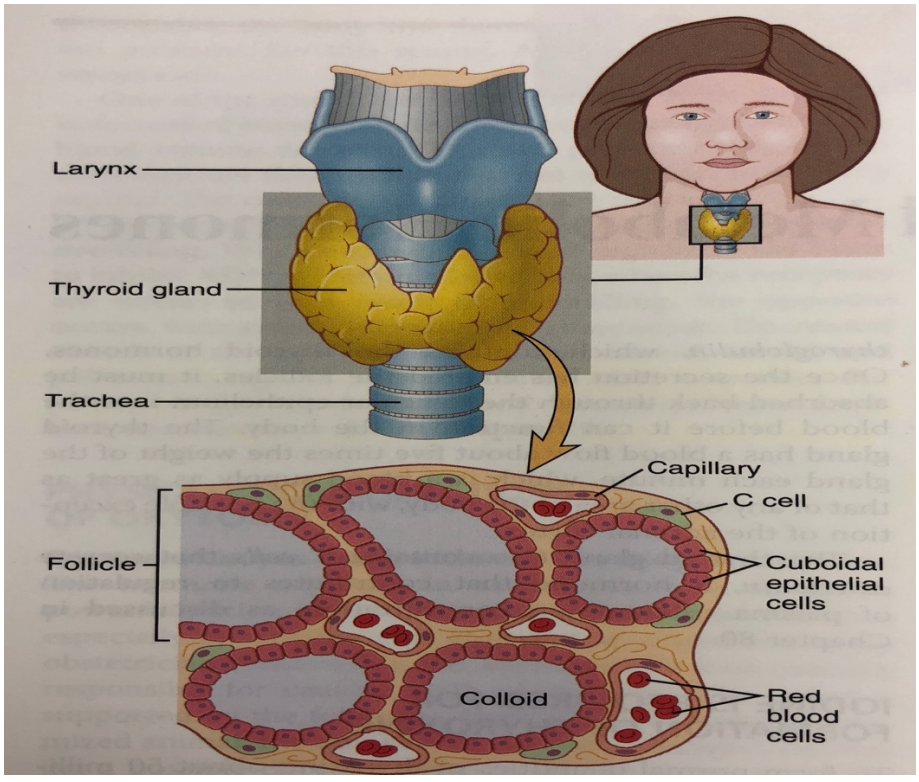

Figure 4: Microscale structure of the human thyroid (from Hall 2016).

Another important function of the follicular cells is that they collect iodine. Iodine must be ingested daily, or about 1 mg/week, so that iodine deficiency does not occur. When iodine is ingested orally it is absorbed from the gastrointestinal tract into the blood. Most of the iodine is secreted through the kidneys but about one-fifth is removed and used for the thyroid gland to synthesize Tg for the formation and release of thyroid hormones (Hall 2016).

The first stage in the formation of these thyroid hormones includes the transport of the iodides from the blood to the thyroid glandular cells and follicles. This is done by actively pumping the iodide into the interior of the cell by the action of sodium-iodide symporter. This co-transports one iodide ion and two sodium ions across the plasma membrane. The energy for this transportation against the concentration gradient is mediated by ATPase pumps, which is a process called iodide trapping. From here, the iodide is then transported out of the thyroid cells and into the follicle, where it binds to tyrosine amino acids (Hall 2016).

The other type of cells that are present in the thyroid gland are parafollicular cells. These are known as C-cells and they are responsible for secreting the hormone calcitonin, which is a hormone that is responsible for the regulation of calcium (Chiasera 2013).

The thyroid gland is also controlled through a feedback system which involves the hypothalamus, the pituitary, and the target gland, otherwise known as the thyroid. The role of the hypothalamus is to produce thyrotropin-releasing hormone (TRH), which is a tripeptide that is secreted into the venous system and then goes into the pituitary gland. Upon reaching the pituitary gland, TRH binds to the receptors of the thyrotroph cells and causes the production and secretion of thyroid stimulating hormone (TSH). TSH then binds to the

receptors in the follicular cells of the thyroid gland, which causes the production and secretion of T_3 and T_4, which is an example of positive feedback. However, negative feedback is also present, in which the hypothalamus and pituitary shut down the production of thyroid hormones. This occurs so that the level of circulating hormones is constantly regulated (Chiasera 2013). The components of the thyroid and their function can be seen in Table 4.

Table 4: The components of a human thyroid and their definition/function (from Chiasera 2013).

Component	Definition/Function
Follicular Cells	Produce the thyroid hormones T_3 and T_4
Parafollicular Cells	Also known as C-cells and they secrete the hormone calcitonin, which regulate calcium
Colloid	Enclosed by the follicles. These contain thyroglobulin.
Thyroglobulin	Glycoprotein that is used to produce the thyroid hormones
Triiodothyronine (T_3)	Hormone that is produced from the follicular cells due to iodide consumption
Thyroxine (T_4).	Hormone that is produced from the follicular cells due to iodide consumption
Capillaries	Responsible for regulating thyroid hormones and have red blood cells inside

Organisms of Study

Wood frogs (*Lithobates sylvatica*) are medium in size, ranging from 35-83mm, and tend to have the coloration of dark brown or tan. They are also unspotted with a distinctive dark mask that covers their eye, which extends from the snout to the top of their forelegs. As for the tadpoles, they are also medium sized and tend to be dark grey or brown in coloration, which can be seen in Figure 5. These tadpoles are considered to be the only species to have this style of coloration in the Smokey Mountains during spring and the early summer. The eggs are bicolored, black and white, and are conceived as a cluster that measures 38-100mm in diameter and contains 2,000-4,000 eggs (Dodd 2004).

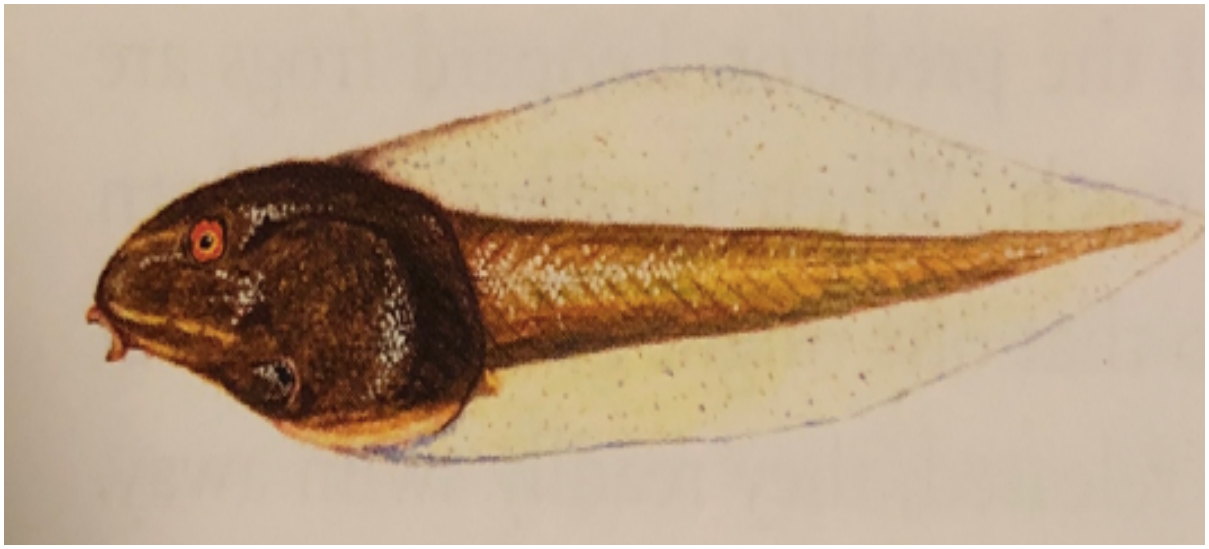

Figure 5: Physical features of a Wood frog (*Lithobates sylvatica*) (From Dodd 2004).

Additionally, the wood frog is considered to be the most widely distributed amphibian in North America. These frogs range from western Alaska, through Quebec and Midwest U.S., to the southern Appalachians (Dodd 2004). A distribution map in the Appalachian Mountains can be seen in Figure 6.

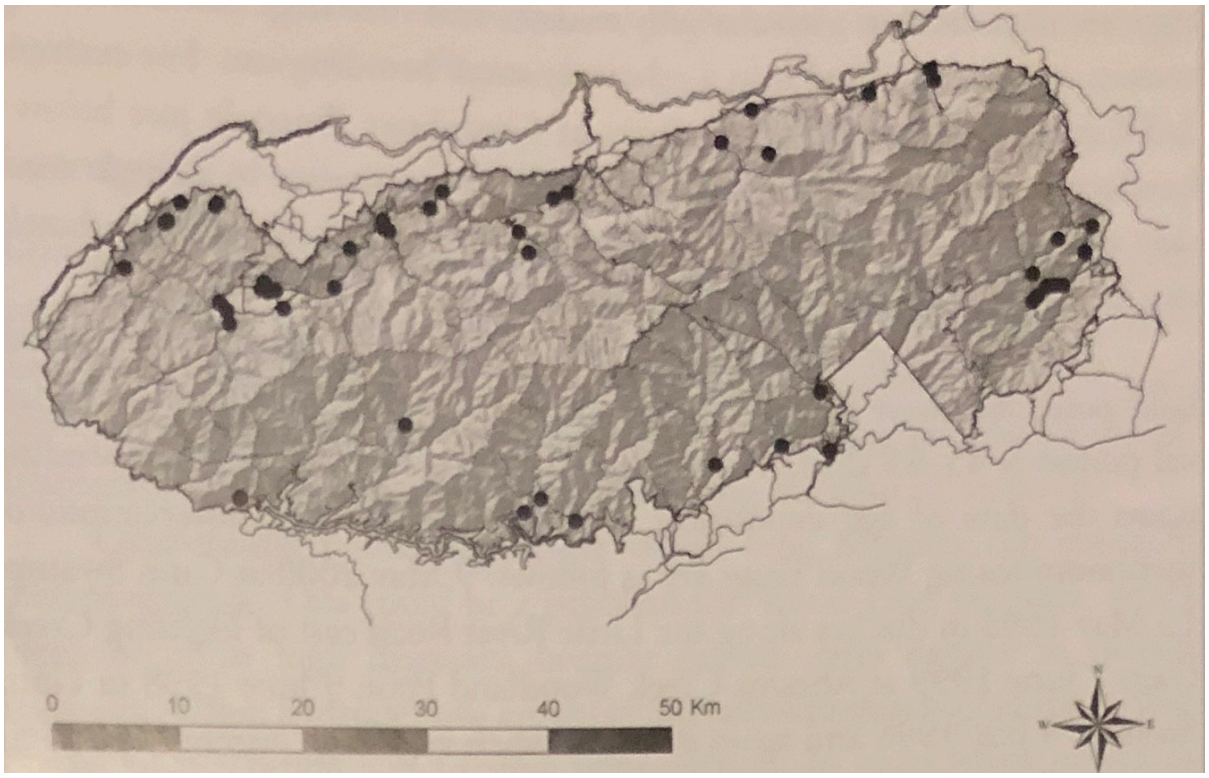

Figure 6: Population distribution of the Wood frog (*Lithobates sylvatica*) in the Appalachian Mountains (from Dodd 2004, Pg. 253).

The breeding period is one of the earliest in the Great Smokey Mountain Region, where the larvae can be found at low level elevations and in any pond or woodland pool. The larvae period can last 45-85 days, and metamorphosis varies depending on the laying of the eggs. When metamorphosis occurs, the tadpoles can grow from 16-18mm, and then feed on the plankton and algae that they are exposed to after birth and periodically consume the jelly masses of other animals (Dodd 2004).

There has been a lack of histological description for the wood frog in recent studies. Most studies have concentrated on the African clawed frog (*Xenopus laevis*), which is a model organism to be used due to its genome being so closely related to human (Hellsten 2010). Due to their similar liver structure, Xenopus will be used as a reference for the histological background of the Wood frog. A normal description of the liver in Xenopus can be seen in Figure 7, while the thyroid can be seen in Figure 8.

A

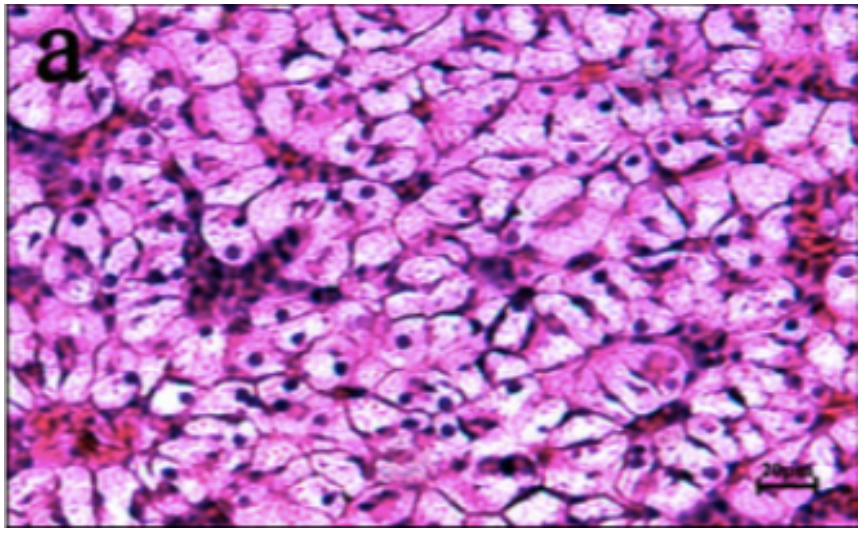

B

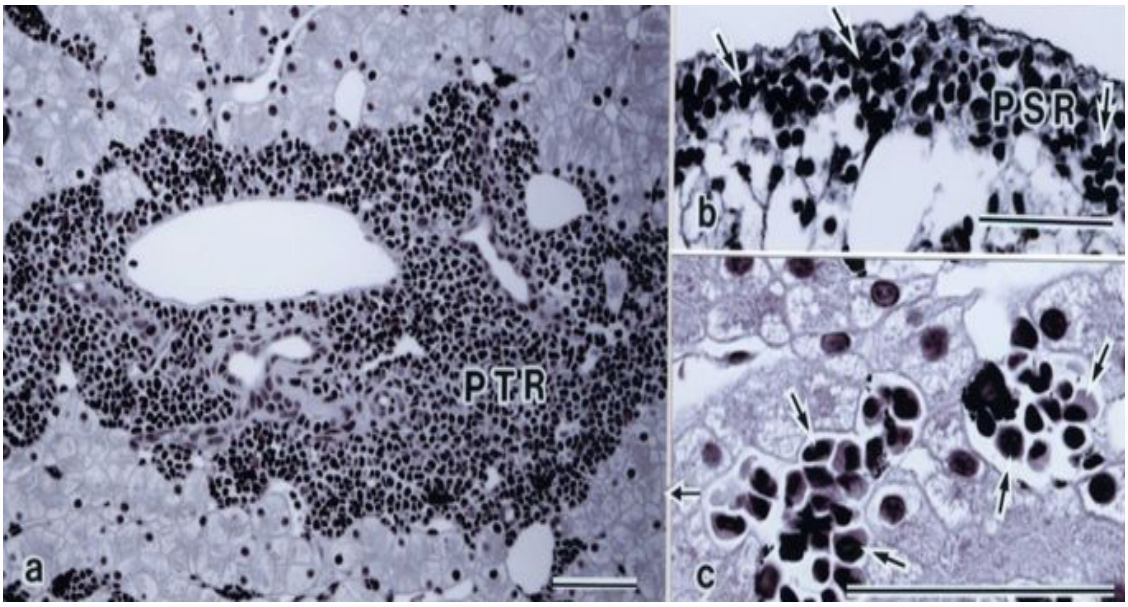

Figure 7: Normal histology of the liver in *Xenopus laevis*. A. (from Lou 2013) B. (from Akiyoshi 2012)

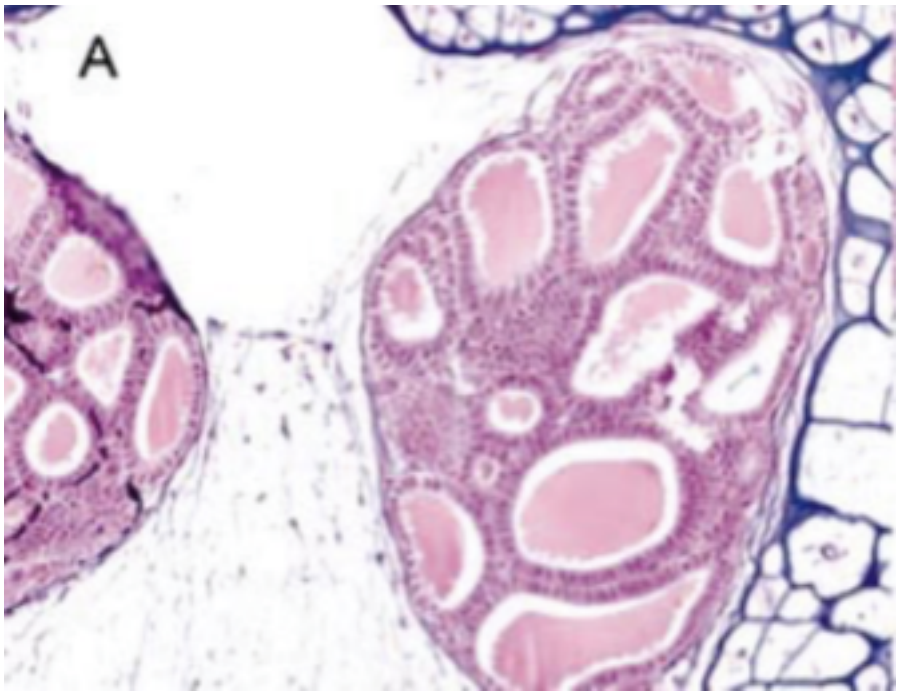

Figure 8: Normal histology of the thyroid in *Xenopus laevis* (from Tietge 2005).

Purpose of Study

The purpose of the study is to identify the acute and chronic effects of CBD exposure on the liver and thyroid structure of wood frogs (*Lithobates sylvatica*). The exposed liver and thyroid will be compared to the liver and thyroid of wood frogs (*Lithobates sylvatica*) that have had no exposure in order to determine the potential changes due to CBD exposure. Additionally, the normal histology of the liver and thyroid of wood frogs will be determined due a lack of research in other studies.

CHAPTER II

MATERIALS AND METHODS

Animals

All care and experimental procedure were approved by MC IACUC approval #202001 (See appendix 1). On February 6, 2020 three clutches of wood frogs (*Lithobates sylvatica*) were obtained from private land in Walland, TN. During collection of the tadpoles, it was raining and the tadpole egg cluster was put into a five gallon bucket filled with water (14°C) from source at 9:20AM. Upon arrival at the study site, three 10 gallon tanks were filled with dechlorinated water and were set to mature to 22°C. After maturing, the tadpole egg cluster was transferred from the buckets to the three 10 gallon tanks. Gosner staging was done (Gosner 1960) and determined the tadpoles to be at stage 21. The tadpoles were left for three days to be able to hatch and eat the algae and egg masses afterwards. After, tadpoles were fed Navisco frog brittle daily and water changes were done as needed.

On February 27, 2020 tadpoles were collected from the same site three clutches in Walland, TN (average outdoor temperature being 33°C and indoor temperature was 22°C) and were placed into three different 10-gallon tanks in the same manner as before. Then on February 28, 2020 the new and old clutch were restaged, and the old tadpoles were found to be at stage 40, while the new tadpoles were found to be at stage 27. The two groups of tadpoles at stage 40 and stage 27 were separated, within their subsets, into Control and

Experimental (CBD exposed) groups by placing 20 tadpoles from each subset into separate tanks specific for either a control group or experimental group. Then, every tadpole from all tanks were reweighed and outliers were replaced with tadpoles of similar weight to the average weight of the tadpoles contained in that tank to make sure consistency was present between feedings. The feeding quantity was also changed for the stage 40 tadpoles to ensure 15mg/kg dosing and feeding quantity was calculated for the stage 27 tadpoles to ensure 15mg/kg dosing.

Preparation of CBD Experimental Feeding

On February 18, 2020 three tadpoles from two of the 10 gallon tanks were weighed and the average weight between all was recorded. Calculations were then performed to determine how much CBD would be needed in order to make 160 servings of food at a 15mg/kg dosing.

For the preparation of the food, on February 21, 2020 80.0g of the Navisco frog brittle and 55.2mg of CBD isolate was placed into a 500mL round bottom flask, then approximately 250mL of 200 proof pure ethanol was added to dissolve the CBD and Navisco frog brittle into solution. The round bottom flask was then rotovapped at 142RPM to dryness. During the rotovapping process, drying was stopped due to time constraints and the round bottom flask was sealed and set out on the lab bench for later use. The next day the food was rotovapped to fully dry.

On February 25, 2020 0.5g of the CBD integrated frog brittle was divided into five different centrifuge tubes. To each of the vials, 3.0mL of HPLC grade methanol was added. Each tube was then vortexed for 30 seconds and placed into a centrifuge for five minutes at 7000RPM. The supernatant was extracted from each tube and transferred into HPLC vials

and the lids were crimped. One of the vials was discarded due to particles still floating around in the supernatant. HPLC was then run to ensure that each feeding had 0.345mg of CBD present per feeding.

Treatment

On March 2, 2020 experimentation began by feeding the experimental stage 40 tadpoles 1/8tsp (approximately 0.5g) of the CBD integrated food brittle, and the control stage 40 tadpoles 1/8tsp (approximately 0.5g) of regular Navisco frog brittle. The experimental stage 27 tadpoles were fed two small plastic spoon scoops (approximately 0.16g) of the CBD integrated food brittle, while the control stage 27 tadpoles were fed the same amount of the Navisco food brittle. Exposure continued for a total of 16 days. On March 16, 2020 a ramp was set up for each of the stage 40 tadpoles so that they would be able to migrate out of the water as they transitioned from the tadpole stage to the frog stage. During experimentation, 10 of the experimental frogs died and 5 of the control frogs died. On March 19, 2020 all tadpoles and frogs were staged (Gosner 1960), reweighed, anesthetized, opened and fixed in Bouin's solution.

Tissue Collection, Fixation, Histology

Each one of the frogs and tadpoles were anesthetized using 0.5g/L of ms-222. This was done by placing them into a shallow dish containing a solution of the ms-222. Once fully anesthetized, all of the tadpoles and frogs were cut open using a scalpel in the frontal abdominal cavity. This was to ensure a clean sight of the liver, as well as to clearly visualize the rest of the abdominal organs and properly fix the tissue.

After this, each of the tadpole and frog bodies were placed into Bouin's fixative so that decay of the tissue could be prevented. Then, the bodies were left in the fixative for

approximately two months. Next, the bodies were dissected in which the livers were removed and placed into separate containers depending on tadpole or frog and control or experimental. The next step was clearing of the fixative, where it was drained and replaced with 70% ethanol. The ethanol was changed daily for two weeks until the fixative was completely cleared out of the bodies and livers.

Histology was then performed to prepare the tissue for slide placement. The first step of the histology process was to embed both the body and the livers of the frogs and tadpoles. Each of the bodies and the livers were placed into their own separate plastic cassettes used for the embedding process, but each cassette contained more than one of the livers or bodies.

The tissues were then to be dehydrated, starting by leaving the cassettes in 70% alcohol overnight. The following protocol was followed where we moved the cassettes over to a new solution: 80% ethanol (1 hour), 95% ethanol (1 hour), 100% ethanol (1 hour), 100% ethanol (1 hour), SafeClear (1 hour), SafeClear 2 (1 hour). After this was completed, the cassettes were moved from the second SafeClear container into a jars of paraffin wax that was placed into a vacuum chamber. The tissue was to be infiltrated by the paraffin wax by the following protocol: Wax I (1 hour @ 12 in. Hg), Wax II (1 hour @ 15 in. Hg), Wax III (1 hour @ 21 in. Hg), Wax IV (1 hour @ 25 in. Hg). Then, all of the cassettes were placed into a paraffin wax pot to ensure that the wax did not harden around the tissue. Each of the cassettes were taken out one by one to then be embedded in their own wax block (Crain 2020).

The tissues were then ready for the sectioning portion of histology where they would be cut and placed on slides. The blocks of wax were trimmed into a pyramid orientation to ensure that it would not break during sectioning. The trimmed wax block was placed into a

microtome and was sectioned at 12µm. The bodies of both the tadpoles and frogs were sectioned until going past the eyes fully. Then, portions from different areas were taken to ensure samples of thyroid was collected. The ribbons of tissues and wax were then floated on a warm water bath that contained a pinch full of gelatin. The ribbons were then mounted onto an accordingly labelled glass slide and set onto a slide warmer until dry. Each slide for the bodies had a total of two ribbons placed on it and the liver slides had two to three ribbons depending on size. Due to improper embedding, there were some of both the frogs tadpoles of the control and experimental that the tissue disintegrated during the sectioning process.

The next day the slides were ready for the staining protocol (Figure 9). The stains used for this protocol were Hematoxylin and Eosin. After the staining was done, a cover slip was applied using Permount and the slides were left to dry overnight before they were analyzed.

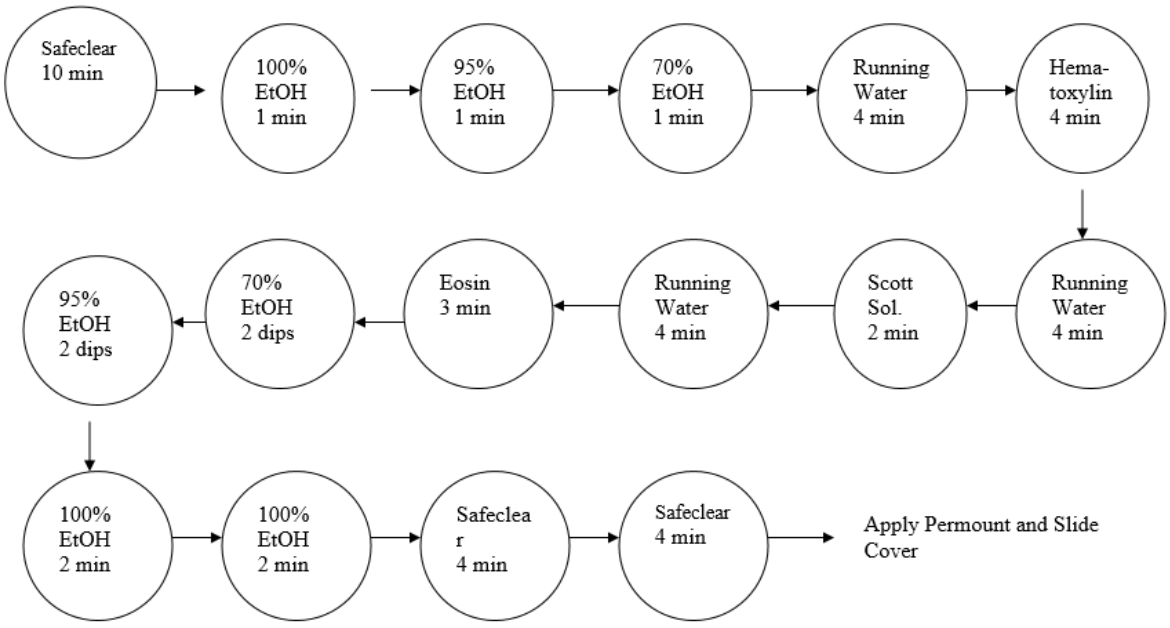

Figure 9: Hematoxylin and Eosin staining protocol that was used to stain both the liver and body tissue of both the frogs and tadpoles (Crain 2020).

Endpoints Measured

The stained liver and thyroid sections were analyzed under a compound microscope. The microscope was calibrated so that there would be consistent measurements taken using a 0.1mm stage micrometer. For the livers, the cells measured were hepatocytes, in which both the height and width were measured. A total of 20 hepatocytes were measured per individual animal. Density of hepatocytes in a given area was also measured, 5 counts per animal. For the thyroid, both follicles and cuboidal epithelial cells were measured. Height and width were taken from each of these and a total of 5 follicles and 10 cuboidal epithelial cells were measured per individual animal.

After measuring with a microscope, the final sample size could be determined. With some slides damaged due to improper cover slip attachment and tissue disintegrating during the sectioning process there were a total of 18 samples of the frog liver control group, 9 of the frog liver experimental group, 17 of the tadpole liver control group, and 12 of the tadpole liver experimental groups. Then for the bodies, there was 10 frog bodies and 20 tadpole bodies in the control group, while there was 10 frog bodies and 20 tadpole bodies in left in the experimental group.

After measuring was completed, photos were taken of both the hepatocytes and thyroids of CBD exposed frogs and tadpoles, as well as non-CBD exposed frogs and tadpoles. Photos of the hepatocytes were each taken at 400X, while photos of the thyroids were each taken at both 100X and 400X.

Statistical Analysis

Statistical analysis was used to determine if there was a significant difference in the length and width of liver hepatocytes, along with the density in a given area. It was also used to determine if there was a significant difference in the length and width of both follicles and cuboidal epithelial cells of the thyroid. Standard errors were taken during the statistical analysis, as well as two-tailed t-tests to determine if there was a significant difference in the length and width of liver hepatocytes, and the length and width of follicles and cuboidal epithelial cells of thyroids.

CHAPTER III

RESULTS

During the dissection stage of the livers in the frog and tadpole bodies, it was seen that almost all the experimental frogs had distinct differences in anatomy. Many experimental frog livers had a portion of the intestines wrapped around their livers. This caused for intensive restraint between the two lobes, and made an hourglass-shaped liver once fully dissected out of the body, almost to the point of separation between the two lobes.

All hepatocyte measurements for both exposed and control frogs and tadpoles are shown in Table 5. Hepatocytes were significantly shorter ($p = <0.0001$) in CBD exposed frogs (18.533µm ± 0.266SE; see photo Figure 10a) compared to the non-CBD exposed wood frogs (31.725µm ± 0.310SE; see photo in Figure 10b), and they were also significantly thinner ($p = <0.0001$) in CBD exposed frogs (19.217µm ± 1.477SE; see photo in Figure 10a) compared to non-CBD exposed frogs (29.125µm ± 0.547SE; see photo in Figure 10b). Tadpoles showed the same results, with significantly shorter ($p = <0.0001$) hepatocytes in CBD exposed tadpoles (22.325µm ± 0.906SE; see photo in Figure 11a) compared to non-CBD exposed wood frog tadpoles (29.869µm ± 0.528SE; see photo in Figure 11b), and significantly thinner ($p = <0.0001$) in CBD exposed tadpoles (19.738µm ± 0.635SE; see

photo in Figure 11a) compared to non-CBD exposed tadpoles (25.059µm ± 0.635SE; see photo in Figure 11b).

Data analysis was also conducted on the density of hepatocyte cells in the liver of wood frogs and tadpoles that were exposed to CBD, compared to ones that weren't exposed to CBD. Hepatocyte density was significantly higher ($p = <0.0001$) in CBD exposed frogs (757.978µm ± 5.125SE; see photo in Figure 10a) compared to non-CBD exposed frogs (594.389µm ± 4.271SE; see photo in Figure 10b). Tadpoles showed the same results, with significantly higher ($p = <0.0001$) hepatocyte density of CBD exposed tadpoles (537.167µm ± 3.964SE; see photo in Figure 11a) compared to non-CBD exposed tadpoles (429.412µm ± 3.983SE; see photo in Figure 11b).

All thyroid measurements for both exposed and control frogs and tadpoles are also shown in Table 5. Both follicles and cuboidal epithelial cells height and width were compared between control and CBD exposed frogs and tadpoles. Follicles were significantly shorter ($p = <0.0001$) in CBD exposed tadpoles (23.400µm ± 0.254SE; see photos in Figure 12a and c) compared to the non-CBD exposed tadpoles (28.410µm ± 0.566SE; see photos in Figure 12b and d), and they were also significantly thinner ($p = 0.004$) in CBD exposed tadpoles (19.530µm ± 2.567SE; see photos in Figure 12a and c) compared to the non-CBD exposed tadpoles (27.330µm ± 0.259SE; see photos in Figure 12b and d). However, the height of cuboidal epithelial cells wasn't significantly shorter ($p = 0.153$) in CBD exposed tadpoles (8.475µm ± 0.057SE; see photos in Figure 12a and c) compared to the non-CBD exposed tadpoles (8.310µm ± 0.098SE; see photos in Figure 12b and d). Although, cuboidal epithelial cells were significantly thinner ($p <0.0001$) in CBD exposed tadpoles (8.325µm ± 0.102SE; see photos in Figure 12a and c) compared to the non-CBD exposed tadpoles

(9.420µm ± 0.098SE; see photos in Figure 12b and d). Follicles were significantly shorter ($p = 0.033$) in CBD exposed frogs (59.580µm ± 3.623SE; see photos in Figure 13a and c) compared to the non-CBD exposed frogs (50.460µm ± 1.578SE; see photos in Figure 13b and d), but they weren't significantly thinner ($p = 0.052$) in CBD exposed frogs (48.660µm ± 2.319SE; see photos in Figure 13a and c) compared to the non-CBD exposed frogs (56.400µm ± 2.918SE; see photos in Figure 13b and d). The cuboidal epithelial cell height was significantly shorter ($p < 0.0001$) in CBD exposed frogs (12.360µm ± 0.417SE; see photos in Figure 13a and c) compared to the non-CBD exposed frogs (8.970µm ± 0.122SE; see photos in Figure 13b and d), but the width wasn't significantly thinner ($p = 0.704$) in CBD exposed frogs (8.070µm ± 0.221SE; see photos in Figure 13a and c) compared to the non-CBD exposed frogs (8.160µm ± 0.075SE; see photos in Figure 13b and d).

Table 5: Mean height, width, and density of hepatocytes in CBD exposed and non-CBD exposed wood frogs and tadpoles, along with corresponding p-values. Mean height and width of follicle and cuboidal epithelial cells in the thyroid of wood frogs and tadpoles, along with corresponding p-values.

	Tadpole Exposed	Tadpole Control	p-value	Frog Exposed	Frog Control	p-value
Hepatocyte height (µm)	22.325 ± 0.906SE	29.869 ± 0.528SE	<0.0001	18.533 ± 0.266SE	31.725 ± 0.310SE	<0.0001
Hepatocyte width (µm)	19.738 ± 0.635SE	25.059 ± 0.635SE	<0.0001	19.217 ± 1.477SE	29.125 ± 0.547SE	<0.0001
Hepatocyte density (# per field of view)	537.167 ± 3.964SE	429.412 ± 3.983SE	<0.0001	757.978 ± 5.125SE	594.389 ± 4.271SE	<0.0001
Thyroid follicle height (µm)	23.400 ± 0..254SE	28.410 ± 0.566SE	<0.0001	59.580 ± 3.623SE	50.460 ± 1.578SE	0.033
Thyroid follicle width (µm)	19.530 ± 2.567SE	27.330 ± 0.259SE	0.004	48.660 ± 2.319SE	56.400 ± 2.918SE	0.052
Thyroid cuboidal epithelial cell height (µm)	8.475 ± 0.057SE	8.310 ± 0.098SE	0.153	12.360 ± 0.417SE	8.970 ± 0.122SE	<0.0001
Thyroid cuboidal epithelial cell width (µm)	8.325 ± 0.102SE	9.420 ± 0.098SE	<0.0001	8.070 ± 0.221SE	8.160 ± 0.075SE	0.704

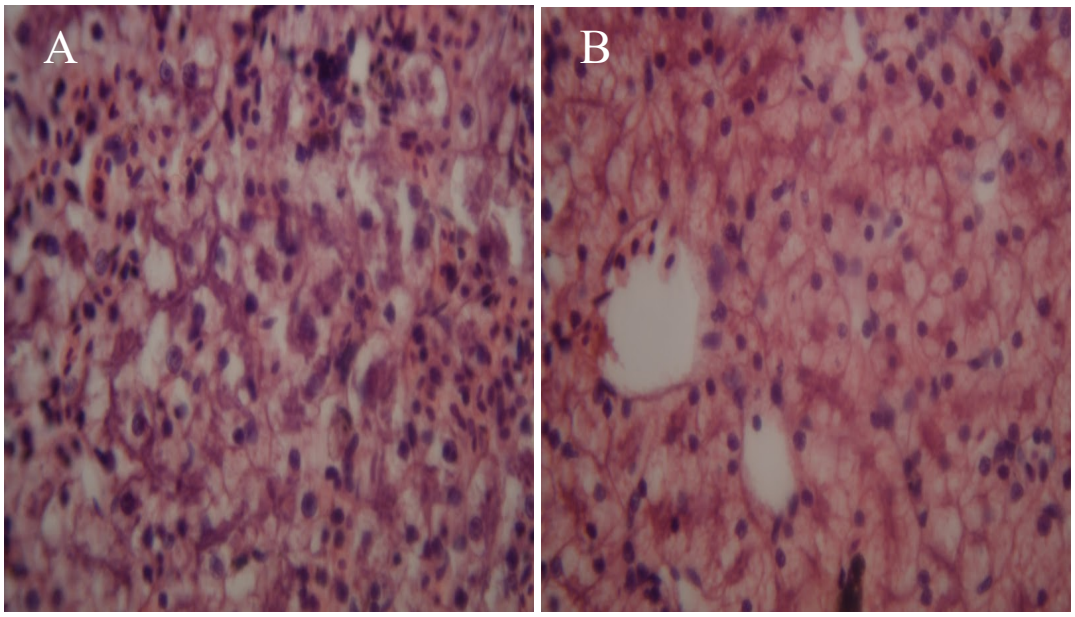

Figure 10: A). Microscopic image at 400X of the hepatocytes in a CBD exposed frog. B). Microscopic image at 400X of the hepatocytes in a non-CBD exposed frog.

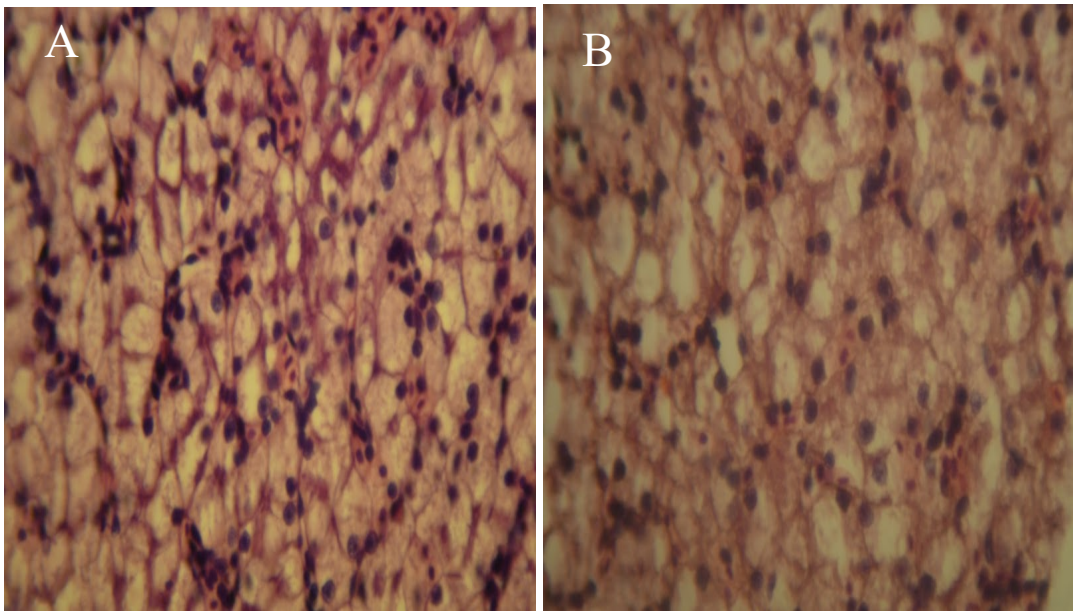

Figure 11: A). Microscopic image at 400X of the hepatocytes in a CBD exposed tadpole. B). Microscopic image at 400X of the hepatocytes in a non-CBD exposed tadpole.

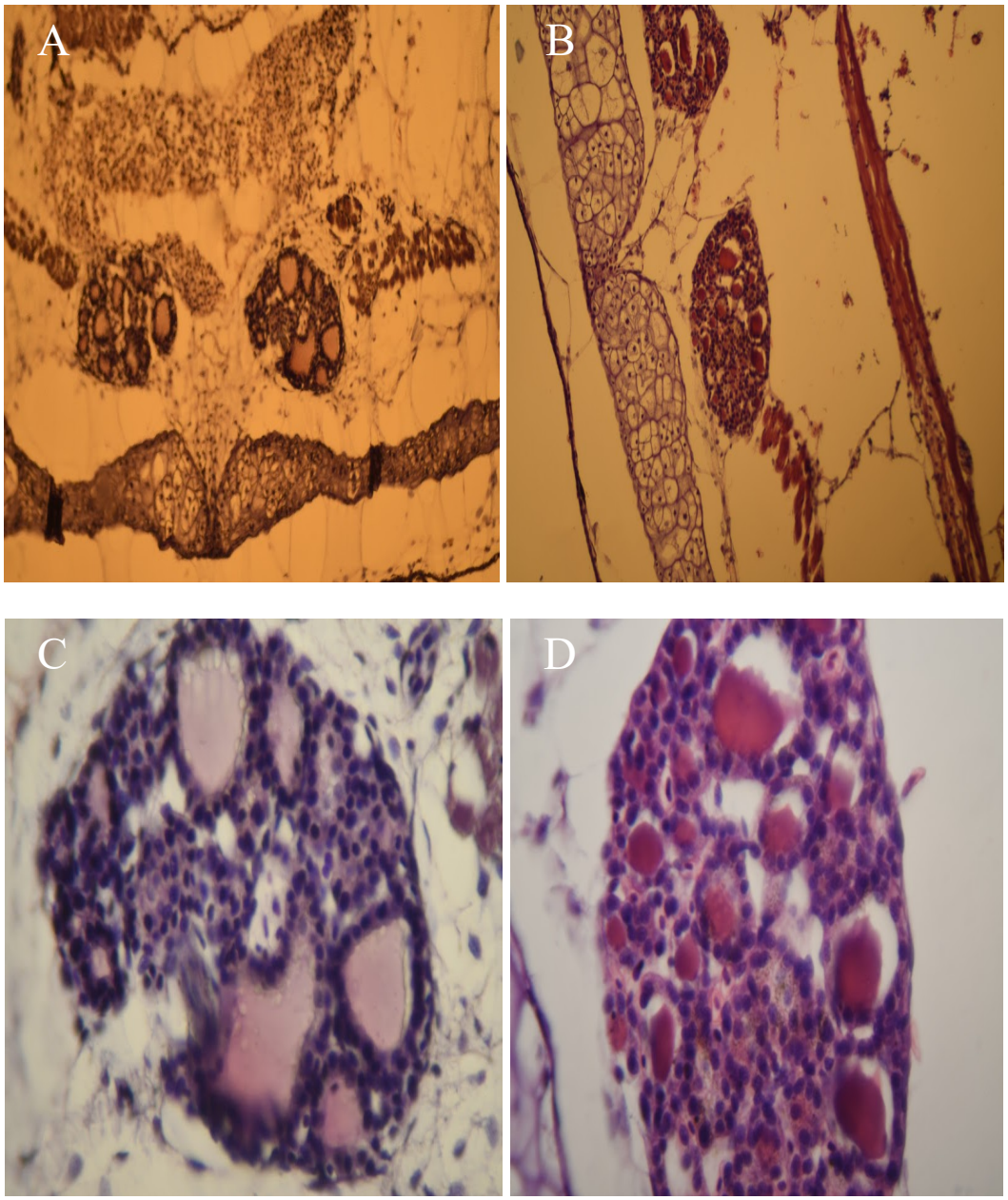

Figure 12: A). Microscopic image at 100X of the thyroid in a CBD exposed tadpole. B). Microscopic image at 100X of the thyroid in a non-CBD exposed tadpole. C). Microscopic image at 400X of the thyroid in a CBD exposed tadpole. D). Microscopic image at 400X of the thyroid in a non-CBD exposed tadpole.

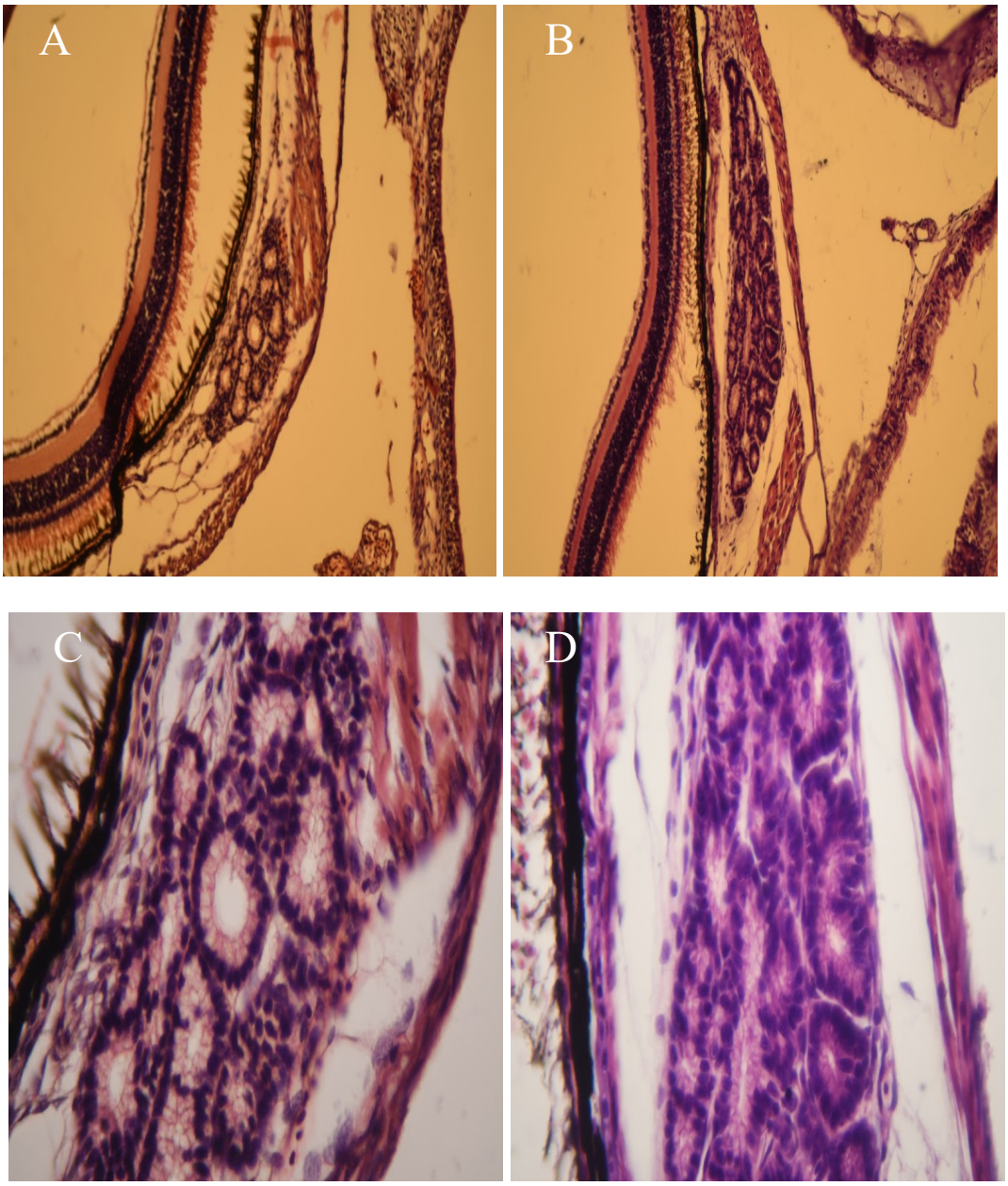

Figure 13: A). Microscopic image at 100X of the thyroid in a CBD exposed frog. B). Microscopic image at 100X of the thyroid in a non-CBD exposed frog. C). Microscopic image at 400X of the thyroid in a CBD exposed frog. D). Microscopic image at 400X of the thyroid in a non-CBD exposed frog.

CHAPTER IV

DISCUSSION

Effects on the Liver

The hepatocytes were significantly smaller in both height and width in tadpoles and frogs for the CBD exposed groups in the present study. Similarly, the introduction of cannabidiol-rich cannabis extract (CRCR) orally in 8-week old mice did have an effect on the liver (Kutanzi 2020). From this exposure, there was an increase in the liver weight and liver-to-body weight ratio. Along with these results they found that CRCE also caused a significant increase in the mRNA levels in seven out of the nine mouse CYP enzymes. This implied that the exposure of CRCE had prolonged effects on hepatic drug metabolizing enzyme activity. With these CYP-associated increases, which is usually due to an adaptive response, it could be inferred that the prolonged exposure to CRCE could lead to decomposition of adaptive responses and result in hepatotoxicity. This could be similar to what is happening in our study, as the CBD exposed frogs demonstrated smaller hepatocytes, which could be affecting the ability of the liver to detoxify substances. Similarly, another study used CBD-enriched cannabis extract and exposed it to an 8-week old set of mice in order to study the acute (2460mg/kg) toxicity effects on the liver (Ewing 2020). In this study, they found an increase in serum ALT, AST, total bilirubin, and intrahepatic concentrations of oxidized glutathione, which implies that there was significant liver injury. Thus, some types of CBD can cause liver defects, and the CBD dosage also can contribute to liver damage.

Agricultural pesticides are toxicants that have shown similar effects. This was seen in a recent study, which demonstrated that frequent exposure to pesticides in farmers caused an increase in ALT, which significantly altered the liver function (Mboe 2020). Since the mentioned toxicants demonstrated the effect of decreasing hepatocyte size, as CBD did in the present study, and that decreased size affected the liver function, it can be inferred that CBD also affected the function of the liver in wood frogs.

The CBD exposed groups also had a higher number of hepatocytes. This implies a possibility that hepatocytes experienced more mitotic events, which caused them to become smaller after each division. This would also explain why there was higher counts of hepatocytes in the CBD exposed group. In relation to the results found in this study, there has been other studies shown to have proliferating hepatocyte effects. One study showed that people with Hepatitis B are given sodium taurocholate cotransporting polypeptide-inhibiting drugs which downregulates the effects of the virus and causes for more proliferating hepatocytes (Yan 2019). CBD could possibly have some similar effects by contributing to the increased activity of proliferation in hepatocytes.

Effects on the Thyroid

For thyroids, follicle height and width of tadpoles, follicle height of frogs, cuboidal epithelial cell width of tadpoles, and cuboidal epithelial cell height of frogs differed in size in the CBD exposed groups. However, follicle width of frogs, cuboidal epithelial cell height of tadpoles, and cuboidal epithelial cell width of frogs all had no difference in size when comparing the CBD exposed and non-CBD exposed groups. There are other recent studies that have shown similar effects to our own study. Monosodium glutamate has been known to be a major flavor enhancer and is used as a food additive, but it has shown to have drastic

effects on the size of follicular cells in rats. The follicles in this study were varying in shape and there was seen to be an increase in height, which could inevitably result in differentiation of function (Rani 2013). Based on the effect that this toxicant showed to have on the thyroid structure, as CBD did in the present study, it could be inferred that CBD also affected the structure and possibly the function of the thyroid.

These results suggest a possibility that both follicle and cuboidal epithelial cells experience higher mitotic events as a result of CBD exposure. Despite this, given that certain cell groups had no significant difference, it could indicate that the tadpoles and frogs did not have an adequate exposure period to the CBD. Overall, a majority of these cells did show growth differences in the CBD exposed groups to a certain extent.

Further Studies

Further studies should be conducted to further discern the effects of CBD on the liver and thyroid. One limitation of the current study was short duration of exposure. A longer exposure period could help determine more statistical differences that CBD could have had on the liver and thyroid that were not seen due to the short exposure time. Also, a larger sample size is needed for future studies, as the sample size in this study was limited due to early mortality, sectioning, and staining flaws.

To expand on the current study, the next step would be to expose African clawed frogs (*Xenopus laevis*) to CBD in order to more directly relate findings to humans, as their genome more similarly resembles that of humans than the wood frogs (*Lithobates sylvatica*) that were studied in the present study. A recent study exposed zebrafish to difenoconazole and they assessed the effect of this on hepatoxicity. RNA sequencing showed differences in the gene expression of the hepatocytes of the zebrafish that were exposed (Jiang 2020).

Future studies should be conducted similarly, in which RNA sequencing could determine possible gene expression differences in frogs exposed to CBD.

Despite the need for further studies, the present study determined that CBD did have an effect on the growth of both the liver and the thyroid of wood frogs and tadpoles (*Lithobates sylvatica*). This could be a building block of future research to determine if the acute and chronic effects of CBD in the liver and thyroid are applicable to humans, as there is a growing importance to understand the effects of CBD due to its growing recreational use in the United States (Hazekamp 2018).

APPENDIX 1: MARYVILLE COLLEGE IACUC APPROVAL

MARYVILLE COLLEGE INSTITUTIONAL ANIMAL CARE & USE COMMITTEE
Application for Use of Vertebrate Animals in Student Research

Provide information after each bold item
Student Name:
Bryan Crouser
Student Email Address:
bryan.crouser@my.maryvillecollege.edu
Date:
2/11/20
Senior Study Advisor:
Dr. Crain
Species to be used:
Rana sylvatica (Wood Frogs)
Age of animals:
Early stage 26-46 tadpoles
Number of animals in study:
100
Duration of study:
Present-May 31 2020
Location of animals during the study (building and room):
Sutton 114

List personnel to call if problems with animals develop:

Name	Daytime Phone	Nighttime Phone	Emergency No.
Bryan Crouser	423-762-5807	423-762-5807	423-715-9335
D. Andrew Crain	8238	292-8737	

What will happen to the animals at the end of the study? If euthanasia is required, state the specific methods.
The animal will be anesthetized using Euthanasia via MS222 500mg/L which will be injected using a syringe through the pectoral muscle. Time will be given for the animals will to become fully unconcious. Then the animals will be disected in which the liver and the thyroid will both be isolated. These organs will then go through the process of histology.

(Do not write below line: For MC IACUC Use)

Maryville College IACUC Approval Number: 202001
Date Approved: 2/24/20
Signed:

WORKS CITED

Akiyoshi H, Inoue AM. Comparative histological study of hepatic architecture in the three orders amphibian livers. Comparative Hepatology. 2012;11(2). doi:10.1186/1476-5926-11-2.

Baranowska-kuczko M, Kozlowska H, Kloza M, Sadowska O, Kozlowski M, Kusaczuk M, Kasacka I, Malinowska B. Vasodilatory effects of cannabidiol in human pulmonary and rat small mesenteric arteries: modification by hypertension and the potential pharmacological opportunities. J Hypertens. 2020;38(5):896-911.

Calcaterra SL, Cunningham CO, Hopfer CJ. The void in clinician counseling of cannabis use. J Gen Intern Med. 2020;35(6):1875-1878.

Carvalho RK, Santos ML, Souza MR, Rocha TL, Guimaraes FS, Ansermo-Franci JA, Mazarao-Costa R. Chronic exposure to cannabidiol induces reproductive toxicity in male swiss mice. J Appl Tocicol. 2018;38(9):1215-1223.

Chandrasoma P, Taylor C. Concise Physiology, 3e. Ch. 42. The liver: I. Structure & function; Infections. 1995.

Chiasera JM. Back to the basics: thyroid gland structure, function and pathology. The American Society for Clinical Laboratory Science. 2013;26(2):112-117.

Crain DA. Animal Physiology 412 Laboratory Manual. Fall 2020. Maryville College.

Davies DG. Distribution of systemic blood flow during anoxia in the turtle, Chrysemys scripta. Respir Physiol 1989;78(3):383-9.

DeRuiter J. Overview, learning objectives, cases and reading material for thyroid section. Hendocrine Pharmacotherapy Module. 2004:1-24.

Dodd CK. The amphibians of the great smoky mountains national park. 2004:251-255.

Esrefoglu M. Architecture of the liver and biliary tract. SMGroup. 2016;1-12.

Ewing LE, Skinner CM, Quick CM, Kennon-McGill S, McGill MR, Walker LA, ElSohly MA, Gurley BJ, Koturbash I. Hepatotoxicity of a cannabidiol-rich cannabis extract in the mouse model. Molecules. 2019;24(9):1694.

Faria SM, Morais Fabricio D, Tumas V, Castro PC, Ponti MA, Hallak JE, Zuardi AW, Crippa JAS, Chagas MHN. Effects of acute cannabidiol administration on anxiety and tremors induced by a simulated public speaking test in patients with parkinson's disease.J Psychopharmacol. 2020;34(2):189-196.

Gosner K. A simplified table for staging anuran embryos and larvae with notes on identification. Hepetologica. 1960;16:183-190.

Hall J, Guyton A. The Liver as an organ. In: Elsevier, editor. Textbook of Medical Physiology. Thirteenth ed. Philadelphia, PA. 2016:881-885

Hazekamp A. The trouble with CBD oil. Medical Cannabis and Cannabinoids. 2018;1:65-72.

Hellsten U, Harland RM, Gilchrist MJ, Hendrix D, Jurka J, et. al. The genome of the western clawed frog xenopus tropicalis. Science. 2010;328(5978):633-636.

Huestis MA, Solimini R, Pichini S, Pacifici R, Carlier J, Busardo FP. Cannabidiol adverse effects and toxicity. Curr Neuropharmacol. 2019;17(10):974-989.

Jagannathan R. Identification of psychoactive metabolites from *cannabis sativa,* its smoke, and other phytocannabinoids using machine learning and multivariate methods. ACS Omega. 2020;5(1):281-295.

Jiang J, Chen L, Wu S, Lv L, Liu X, Wang Q, Zhao X. Effect of difenoconazole on hepatotoxicity, lipid metabolism and gut microbiota in zebrafish (Danio rerio). Environ Pollut. 2020;265: doi: 10.1016/j.envpol.2020.114844.

Kalra A, Tuma F, Yetiskul E, Wehrle CJ. Physiology, liver. StatPearls Publishing. 2020.

Khan AU, Anjos-Garcia TD, Sobrinho LLF. Cannibidiol-induced paincolytic-like effects and dear-induced antinociception impairment: the role of the CB1 receptor in the ventromedial hypothalamus. Psychopharmacology. 2020;237: doi:10.1007/s00213-019-05435-5.

Kozela E, Kos T, Vogel Z, Krawczyk M, Juknat A, Popik P. Cannabidiol improves cognitive impairment and reverses cortical transcriptional changes induced by ketamine, in Schizophrenia-like model in rats. Molecular Neurobiology. 2019;57(5090):1-15.

Kutanzi KR, Ewing LE, Skinner CM, Quick CM, Kennon-McGill S, McGill MR, Walker LA, ElSohly MA, Gurley BJ, Koturbash I. Safety and molecular-toxicological implications of cannabidiol-rich cannabis extract and methylsulfonylmethane co-administration. International J of Molecular Sciences. 2020;21(20):7808.

Laczkovics C, Kothgassener OD, Felnhofer A, Klier CM. Cannabidiol treatment in an adolescent with multiple substance abuse, social anxiety and depression. Neuropsychiatr. 2020: doi:10.1007/s40211-020-00334-0.

Landmark CJ, Brandi U. Pharmacology and drug interactions of cannabinoids. Epileptic Disord. 2020;22(S1):16-22.

Lattanzi S, Brigo F, Trinka E, Zaccara G, Striano P, Del Giovane C, Silvestrini M. Adjunctive cannabidiol in patients with dravet syndrome: a systematic review and meta-analysis of efficacy and safety. CNS Drugs. 2020;34(3):229-241.

Lazarini-Lopes W, Junior R, Garcia-Cairasco N. The anticonvulsant effects of cannabidiol in experimental models of epileptic seizures: From behavior and mechanisms to clinical insights. Neuroscience & Biobehavioral Reviews. 2020;111:166-182.

Lou QQ, Zhang YF, Zhou Z, Shi YL, Ge YN, Ren DK, Xu HM, Zhao YX, Wei WK, Qin ZF. Effects of perfluorooctanesulfonate and perfluorobutanesulfonate on the growth and sexual development of xenopus laevis. Ecotoxicology. 2013;22(7):1133-1144.

Mabou TA, Marino F, Legnaro M, Luini A, Pacchetti B, Cosentino M. A novel standardized *cannabis sativa* L. extracts and its constituent cannabidiol inhibit human polymorphonuclear leukocyte functions. Int J mol Sci. 2019;20(8):1833.

Mathews NM. Prohibited contaminants in dietary supplements. Sports Health. 2018;10(1):19-30.

Mboe SA, Manfo FPT, Nantia EA, Ngoula F, Telefo PB, Moundipa PF, Cho-Ngwa F. Evaluation of the effects of Agro Pesticides use on liver and kidney function in farmers from Buea, Cameroon. J of Toxicology. 2020;(10):1-10.

Rani P, Khatri K, Chauhan R. Monosodium glutamate induced histomorphometric changes in thyroid gland of adult wistar rat. J of Medical & Allied Sciences. 2013;3(2):67-71.

Ronis MJJ, Pedersen KB, Watt J. Adverse effects of nutraceuticals and dietary supplements. Annu Rev Pharmacol Toxicol. 2018;58:583-601.

Sarris J, Sinclair J, Karamacoska D, Davidson M, Firth J. Medial cannabis for psychiatric disorders: a clinically-focused systematic review. BMC Psychiatry. 2020;20(1):24.

Tietge JE, Holcombe GW, Flynn K, Kosian PA, Anderson LE, Korte JJ, Wolf DC, Degitz SJ. Metamorphic inhibition of xenopus laevis by sodium perchlorate: effects on development and thyroid histology. Environmental Toxicology and Chemistry. 2005;24(4):926-933.

Trefts E, Gannon M, Wasserman DH. The liver. Curr Biol. 2017;27(21):1147-1151.

Vaissi S, Parto P, Sharifi M. Anatomical and histological study of the liver and pancreas of two closely related mountain newts *Neurergus microspilotus* and *N. kaiseri*. Zoologia (Curitiba). 2017;34:1-8.

Yan Y, Allweiss L, Yang D, Kang J, Wang J, Qian X, Zhang T, Liu H, Wang L, Liu S, Sui J, Chen X, Dandri M, Zhao J, Lu F. Down-regulation of cell membrane localized NTCP expression in proliferating hepatocytes prevents hepatitis B virus infection. Emerging Microbes & Infection. 2019;8(1):870-894.